Yüzüncü Yıl Üniversitesi
Fen Bilimleri Enstitüsü Dergisi

Research Article

Investigation of Some Physical Properties of CoAsS Crystal Under Pressure

Ferhat ARSLANBAŞ[1], Emel KİLİT DOĞAN*[1]

[1]Van Yüzüncü Yıl Üniversitesi, Fen Fakültesi, Fizik Bölümü, 65080, Van, Türkiye
Ferhat ARSLANBAŞ, ORCID No: 0000-0002-9835-9745, Emel KİLİT DOĞAN, ORCID No: 0000-0001-7609-7206
*Corresponding author e-mail: ekilit@yyu.edu.tr

Abstract: Density functional theory (DFT) within the generalized gradient approximation (GGA) was used to inquire the structural, electronic, optical, elastic and thermodynamic properties of CoAsS crystal for the ground state (P=0 GPa) and for some pressure values such as 10, 20, 30, 40 and 50 GPa. CoAsS crystal has a semiconductor character with 1.06 eV indirect band gap. By increasing the pressure on CoAsS crystal band gap values were increasing as expected but by 40 GPa band gap value intented to decrease because of the structural deformation caused by the high pressure. The graphs of electronic band structure, density of states, and the all graphs for optic and thermodynamic properties were plotted with all pressure values and given in one figure to provide an easy comparison. Elastic properties were also given to show the effect of pressure on CoAsS crystal. It was noticed that cubic CoAsS mineral was fragile.

CoAsS Kristalinin Bazı Fiziksel Özelliklerinin Basınç Altında İncelenmesi

Öz: CoAsS kristalinin temel durumdaki (P=0 GPa) ve 10, 20, 30 ve 40 GPa basınçları altındaki yapısal, elektronik, optik, elastik ve termodinamik özellikleri Yoğunluk Fonksiyoneli Teorisi ile Genelleştirilmiş Gradyent Yaklaşımı altında incelenmiştir. CoAsS kristali 1.06 eV luk doğrusal olmayan band aralığı ile yarıiletken bir karaktere sahiptir. CoAsS üzerindeki basınç artırıldığında kristal bant aralığı beklendiği gibi artmakta ancak yüksek basıncın neden olduğu yapısal deformasyon nedeniyle 40 GPa değerinden itibaren bant aralığı düşme eğilimindedir. Elektronik bant yapısının grafikleri, durum yoğunluğu, optik ve termodinamik özellikler için tüm grafikler, tüm basınç değerleri ile çizilip, kolay bir karşılaştırma sağlamak için tek bir figürde verilmiştir. Basıncın CoAsS kristali üzerindeki etkisini göstermek için elastik özellikler de verilmiştir. Kübik CoAsS mineralinin kırılgan olduğu bulunmuştur.

1. Introduction

Cobaltite (sulfarsenide of cobalt) is a mineral, composed of cobalt (Co), arsenic (As) and sulfur (S) with the chemical formula CoAsS. It is found in a variety of ore deposits especially in high temperature veins or in metamorphosed rocks. These minerals constitute with a major part of technologically important cobalt deposits especially in Morocco, Canada, US, and Russia (Ertseva, 2002). This mineral is strategically important because of containing cobalt element.

There are different types of cobaltites with different space groups, such as Pca2₁, P2₁3 and Pca2₁ with different crystal structures as orthorhombic, cubic and monoclinic, respectively (Bayliss, 1982). CoAsS in general has a pyrite type structure (Mosselmans, 1995) such as NiAsS (gersdorffite), NiSbS (ullmannite), CoPS, and large number of others (Pielnhofer, 2015; Gao, 2017).

CoAsS has an forceful spin-orbit coupling and because of that it shows magnetocrystalline anisotropy energy (Liu, 2019). CoAsS is an isoelectronic compound (Pielnhofer, 2015) and exhibits ferromagnetism and piezoelectricity. Materials with both ferromagnetism and piezoelectricity are quite beneficial for magnetoelectric memory devices (Liu, 2019). At higher temperatures as 850 ^{0}C, arsenic and sulfur become completely disordered (Weihrich, 2004), because of its functional and adjustable properties, CoAsS is used in a large application fields such as photovoltaics, electrocatalysis and energy storage (Gao, 2017).

Ertseva and Tsymbulov (Ertseva, 2002) studied phase transformations with respect to thermal influences. Many cobaltite specimens from localities in North America, Australia, and Sweden were analyzed with experimental techniques by Bayliss (Bayliss, 1982) in order to investigate the structural properties. Mosselmans et al. (1995) presented metal K- and L3-, sulfur K- and arsenic K- and L3-edge X-ray absorption spectra of a series of metal disulfides, such as FeS₂, CoS₂, NiS₂, and CuS₂, and their isomorphs, FeAsS and CoAsS. Liu and Zhuang have studied the magnetic and phonon properties of single layer ferromagnetic and piezoelectric CoAsS crystal (Liu, 2019). Fleet and Burns (Fleet, 1990) have studied twin boundaries that are incoherent and coherent toward X-ray diffraction in cobaltite. Kaur and Bera (Kaura, 2017) theoretically investigated the effect of alloying on the thermal conductivity and the thermoelectric properties of cobaltite, CoAsS. Here, we studied on cubic CoAsS in order to understand the effect of pressure on structural, electronic, optical, elastic and thermodynamic properties. First, we investigated these properties for the ground state (P=0GPa). Then we examined the effect of pressure for the values of 10, 20, 30, 40 and 50 GPa theoretically on those physical properties, using the Density Functional Theory (DFT) within the Generalized Gradient Approximation (GGA) by ABINIT (Gonze, 2002) computer programme. The motivation of this study is to show the effect of the pressure on the electronic band structure, density of states, real and imaginary parts of dielectric constants, reflectivity, refractive index, extinction coefficients, absorption coefficients, energy-loss function for volume, effective number of valence electrons per unit cell, Helmholtz free energy, internal energy, entropy and constant-volume specific heat for cubic CoAsS compound. The objective of this paper was studying of the optical, elastic and thermodynamic properties of CoAsS for the ground state and the pressure effect on the physical properties for the first time.

2. Materials and Methods

In order to understand the physical properties of CoAsS in the ground state and under pressure we performed a first-principle calculations using ABINIT (Gonze, 2002) code under GGA. There are some types of CoAsS with different crystal structures, however, in this study we investigated the cubic structure with P2₁3 space group (No:198) which has 12 atoms in its unit cell. To perform the calculations under the DFT, the Kohn–Sham (Kohn, 1965) equations were solved using the conjugate gradient minimization method (Payne, 1992). The exchange correlation energy was evaluated by the GGA within the Perdew–Burke–Enzerhof (PBE) (Perdew, 1992) parameterization. The self-consistent FHI (Fritz Haber Institute)-type (Fuch, 1999) norm-conserving pseudopotentials were used with the Troullier-Martins scheme (Troullier, 1991) for the GGA pseudo-potentials of Co, As and S elements. To perform the electronic wave functions, the plane waves were used as the basis set. Co ($3s^2$ $3p^6$ $4s^2$ $3d^7$), As ($4s^2$ $3d^{10}$ $4p^3$) and S ($3s^2$ $3p^4$) states were considered as the true valence states. We performed the optimization of the cut-off energy and the number of k-points and computed the cut-off energy as 30 Hartree and the number of k-points as 45 within the 8 x 8 x 8 Monkhorst-Pack mesh grid (MP) (Monkhorst, 1976) for cubic CoAsS compound.

3. Reults
3.1. Structural properties

Cobaltite, CoAsS, in cubic phase with space group of $P2_13$ (No: 198) was investigated in this research. First, the structural properties were examined in the ground state and under pressure values of P=0, 10, 20, 30, 40 and 50 GPa. The internal atomic coordinates for each pressure were relaxed. All physical properties of a material are directly related with the total energy. For the ground state (for P=0 GPa) the total energy of CoAsS was -172.4521 Hartree. At this total energy value, CoAsS was stable for the ground state, and its volume was 1152.65 $(Bohr)^3$ $(=609\ (Å)^3)$. The lattice parameters were calculated for all pressure values and the ground state (Table 1). For the ground state the lattice parameter was calculated as 10.4849 Bohr (=5.5482 Å) which is very close to the value in the literature, 5.584 Å (Jain, 2013) for the ground state. The lattice parameter values for the P=10, 20, 30, 40 and 50 GPa pressure values could not compared with the literature since there is no any theoretical or experimental data for those pressure values.

Table 1. The volume and lattice parameters of CoAsS with respect to the pressure values

Pressure (GPa)	Volume $(Bohr)^3$	Lattice Parameter (Bohr)
P=0 (Ground State)	1152.65	10.4849
P=10	1089.47	10.2897
P=20	1042.46	10.1395
P=30	1002.78	10.0092
P=40	970.06	9.8991
P=50	944.86	9.8127

As noticed from Table 1, with the increasing of the applied pressure, the volume and the lattice parameters were decreased as expected.

3.2. Electronic properties

To investigate the electronic properties of CoAsS compound, we computed and calculated the electronic band structure and the density of states graphs of cobaltite for ground state and for other all pressure values mentioned before. The electronic band structure graph is obtained for the $\Gamma - X - M - R - \Gamma - M$ high symmetry points and given in Figure 2, with the density of states graph attached (Figure 1(a)), and the detailed part of the electronic band graph between the 0 and 6.5 eV energy interval (Figure 1(b)). The density of states (DOS) values are given in arbitrary units. The Fermi level is adjusted to 0 eV. So the energy levels under the 0 eV (Fermi level) are valence energy levels and the energy levels above the 0 eV are conduction bands. Also from Figure 1 (a), core electron energy levels can be seen. The obtained result for the indirect band gap is 1.0583 eV for ground state, so cubic CoAsS has a semiconducting structure. The band gap values found in the literature are 0.75 eV (Kaura, 2017) and 0.849 eV (Jain, 2013). Figure 1 (a) shows that the main contribution for the density of states comes from the valence bands. After these, we calculated the electronic band structures for different pressure values such as P=10, 20, 30, 40 and 50 GPa. We gave the highest valence and the lowest conduction levels of all pressure values in order to compare the band gaps of CoAsS in all pressure values (Figure 2). The band gap values of the applied pressure values were given in Table 2. In Table 2, it was noticed that the band gap values were increasing with the increasing of the applied pressure values such as 10, 20 and 30 GPa. It is known that when pressure increases, value of band gap also increases (Erdinc, 2015), or when pressure increases the band gap decreases (Okoye, 2004), in other words there is a linear relationship between pressure and band gap. For CoAsS from 0 to 30 GPa, the band gap was increasing with the increasing of the pressure while the band gap was decreasing as the pressure was increasing for 40 and 50 GPa. We noticed that around 40 GPa pressure value the structural deformation occured for cubic CoAsS because of high pressure effect. CoAsS deformed around 40 GPa. Because of that for 40 and 50 GPa pressure values some physical properties such as elastic properties were corrupted. In the following parts we discussed this circumstance in the elastical properties point of view. Also the elastic properties were deformed with the 40 and 50 GPa values.
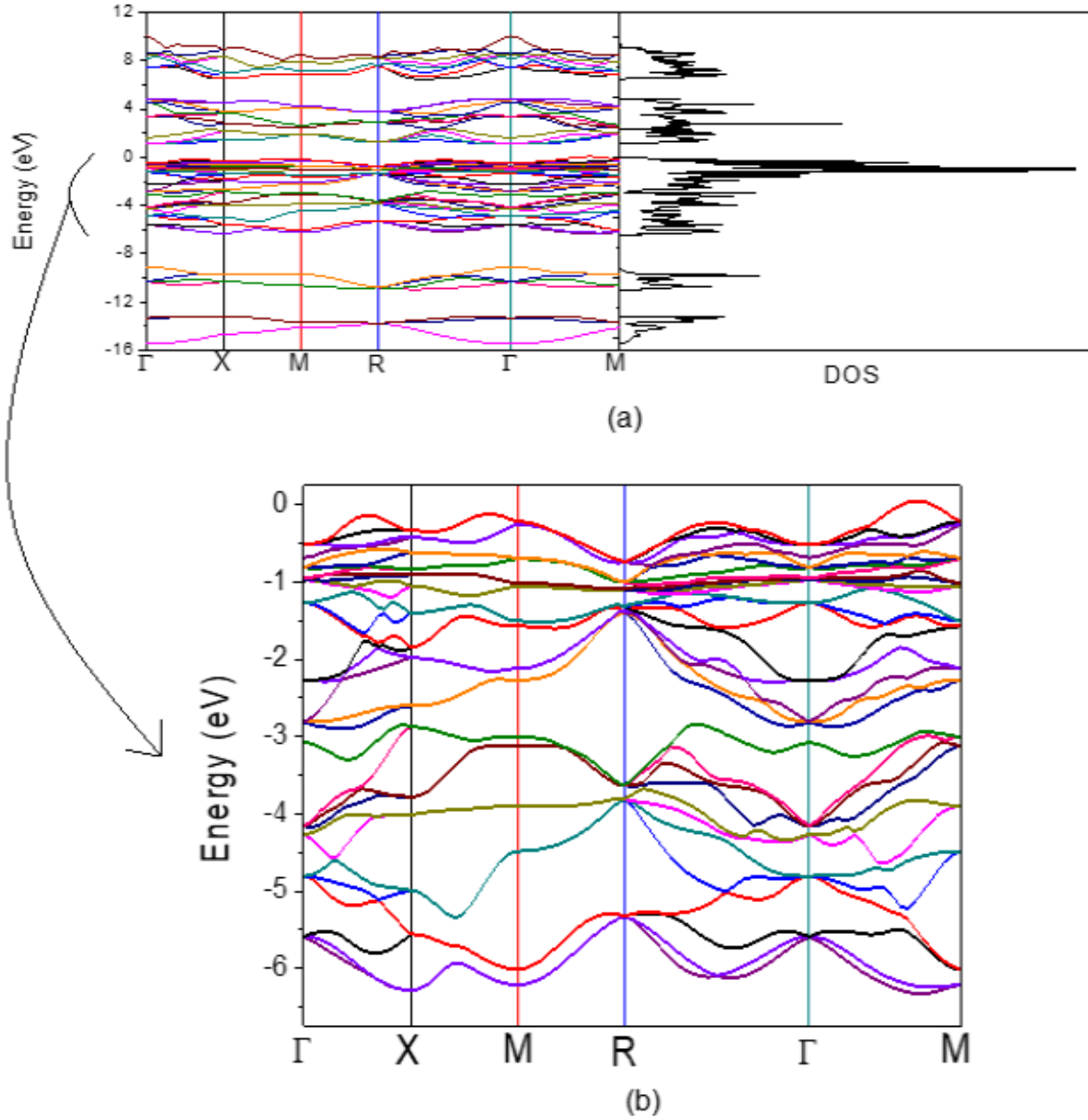
Figure 1. (a) The electronic band structure attached with the total density of states, (b) the detailed part of the valence bands with the 0-6.5 eV energy interval.

Table 2. The band gap values of CoAsS with respect to the pressure values

Pressure (GPa)	Energy Band Gaps (eV)
P=0	1.0583
P=10	1.1637
P=20	1.2084
P=30	1.2367
P=40	1.2317
P=50	1.1577
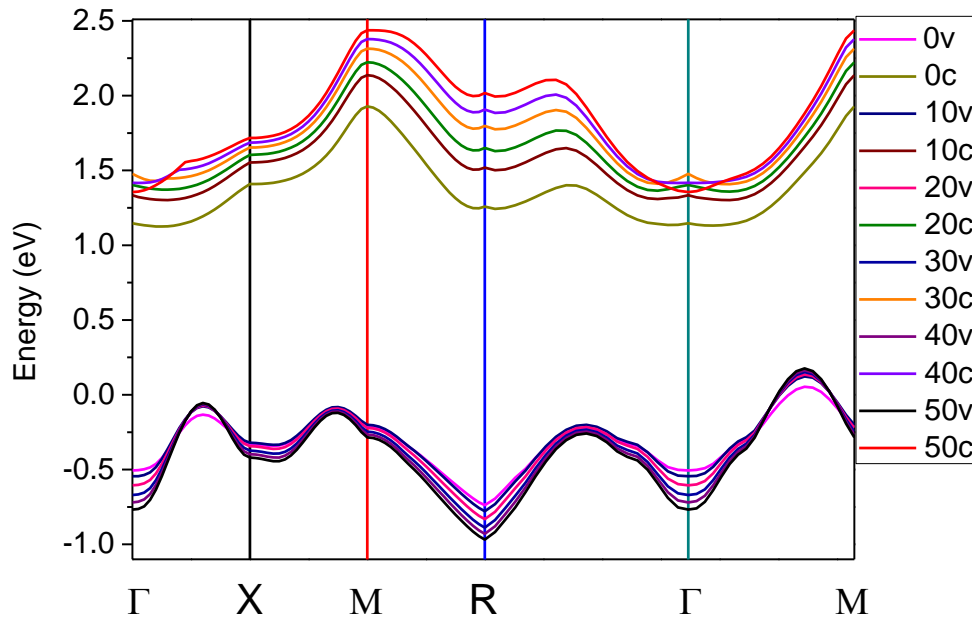
Figure 2. The highest valence and the lowest conduction bands of CoAsS with respect to all applied
pressure values.

Table 3. Energy dispersion of the highest valence band and the lowest conduction band of CoAsS at
various pressures. Energy values are given in eV units

0 GPa	10 GPa	20 GPa	30 GPa	40 GPa	50 GPa	0 GPa
$E_{\Gamma-\Gamma}$	1.6452	1.8683	2.0000	2.1258	2.147	2.1217
E_{X-X}	1.7334	1.8673	1.9476	2.0295	2.0822	2.1338
E_{M-M}	2.1267	2.3417	2.4461	2.5576	2.6468	2.7178
E_{R-R}	1.9899	2.293	2.4694	2.6651	2.8354	2.9854
$E_{\Gamma-X}$	1.4739	1.6443	1.7395	1.8338	1.8216	1.779
$E_{\Gamma-M}$	1.3563	1.5277	1.6209	1.7091	1.6918	1.6361
$E_{\Gamma-R}$	1.8764	2.1045	2.2281	2.3468	2.3508	2.3295
E_{X-M}	1.6158	1.7507	1.829	1.9048	1.9524	1.9909
E_{X-R}	2.1359	2.3275	2.3262	2.5425	2.6114	2.6843
E_{M-R}	2.6468	2.9185	3.0533	3.1953	3.3058	3.4112

In Table 3, the effect of high pressure (40 and 50 GPa) can be seen.
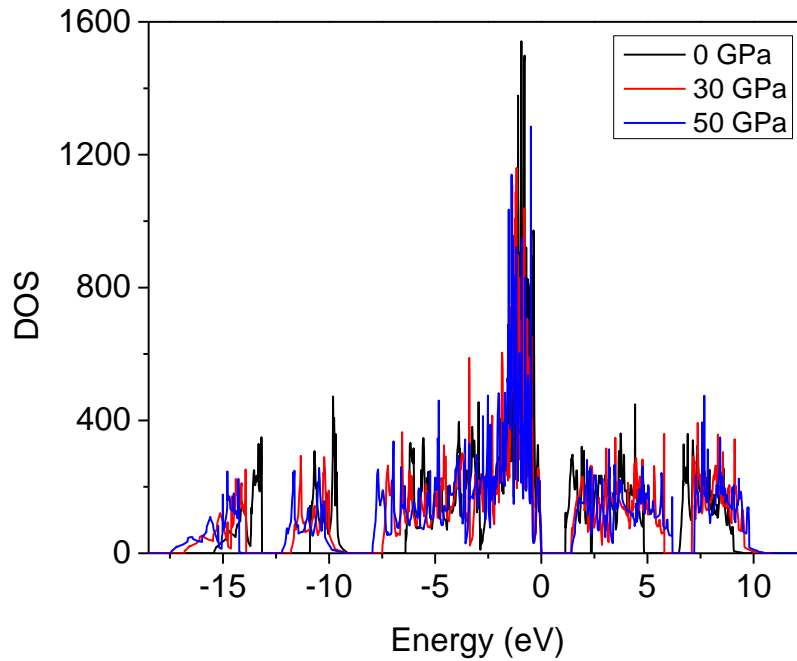
Figure 3. Density of states according to various pressure values.

The density of states graphs for different pressures were given in one plot as seen in Figure 3. This investigation was also done for all pressure values mentioned before, but in the graph only the P=0, 30 and 50 GPa values were given in order to avoid confusion in the figure. As the pressure increased, the frequency values of the valence bands decreased and the frequency of the conduction bands increased, so that the band gap increased up to 40GPa, and decreased for the 40 and 50 GPa, because of the structural and elastical deformation.

The effect of the pressure on the electronic band structure and density of states are done for the first time in the literature with this study.

3.3. Optical properties

To investigate the optical properties, the complex dielectric function should be calculated. The complex dielectric function has the real (ε_1) and the imaginary (ε_2) parts. After calculating the imaginary part of the complex dielectric function, the real dielectric part can be calculated from imaginary part by using the Kramers-Kronig relations. The real part is mostly related with the physical properties of the material and the imaginary part is mostly related with the energy loss of photons in a material, electron transition between electronic bands and optical response of the material such as absorption, reflection etc. with respect to the phonon energies. The complex dielectric function has three different components along the 100, 010 and 001 crystal axes directions. Since cubic materials are optically isotropic, means that the optical responses of polarized light is same for these three directions, only one independent component is sufficient to investigate.

The real and imaginary parts of the dielectric function for P=0, 10, 20, 30, 40 and 50GPa pressure values are given in Figure 4 (a) and 4 (b), respectively.
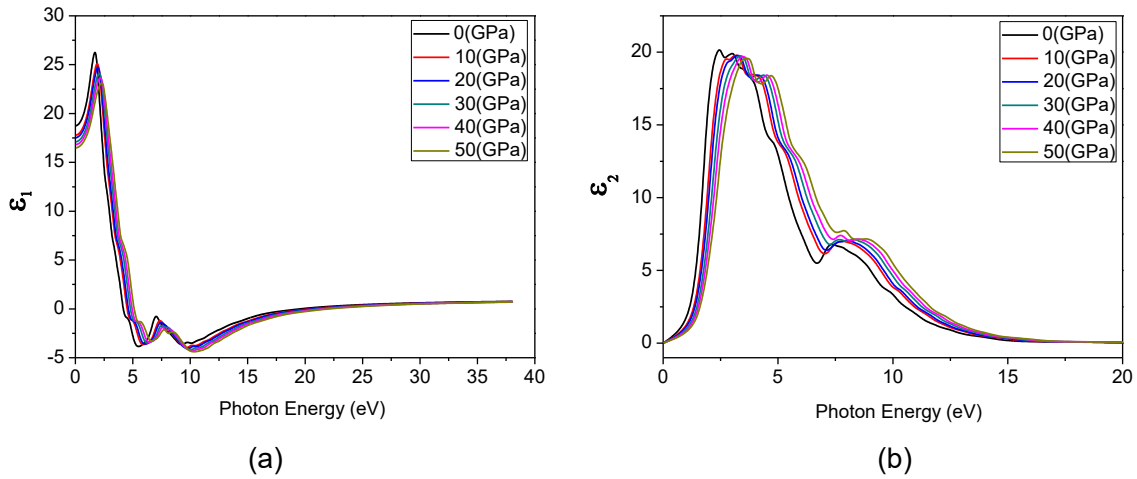
Figure 4. The (a) real and (b) imaginary parts of complex dielectric function under P=0, 10, 20, 30, 40 and 50 GPa pressure values.

The calculated static dielectric constants (ε_0) of cubic CoAsS were 18.75, 17.79, 17.52, 17.11, 16.82 and 16.49 for P=0, 10, 20, 30, 40 and 50GPa, respectively. The negative values of the real dielectric constants were between 4.12-19.83 eV of phonon energies (for P = 0 GPa), that in these intervals the incident electromagnetic waves are totally reflected. This interval was getting enlarged as the pressure increases. Beyond these intervals there was no transition occurs between the states. At the boundary points of these intervals, the zero values of ε_1 corresponds to the plasmon excitations. The parts in which ε_1 increases with the phonon energy is called normal dispersion state, decreasing with the phonon energy is called abnormal dispersion state. From ε_2, for the ground state, between the 0 and 1.06 eV phonon energy interval, there was no absorption but small reflectivity occured because this region showed high transparency. From 1.06 to 2.39 eV there was strong absoption and appreciable reflection. For higher values than 1.06 eV (equal to band gap value, obtained by the electronic band structure graph) the transitions from valence to conduction bands were seen. From 2.39 to 7.39 eV there was high reflectivity. For higher pressure values those energy intervals can be seen from Figure 4 (b).
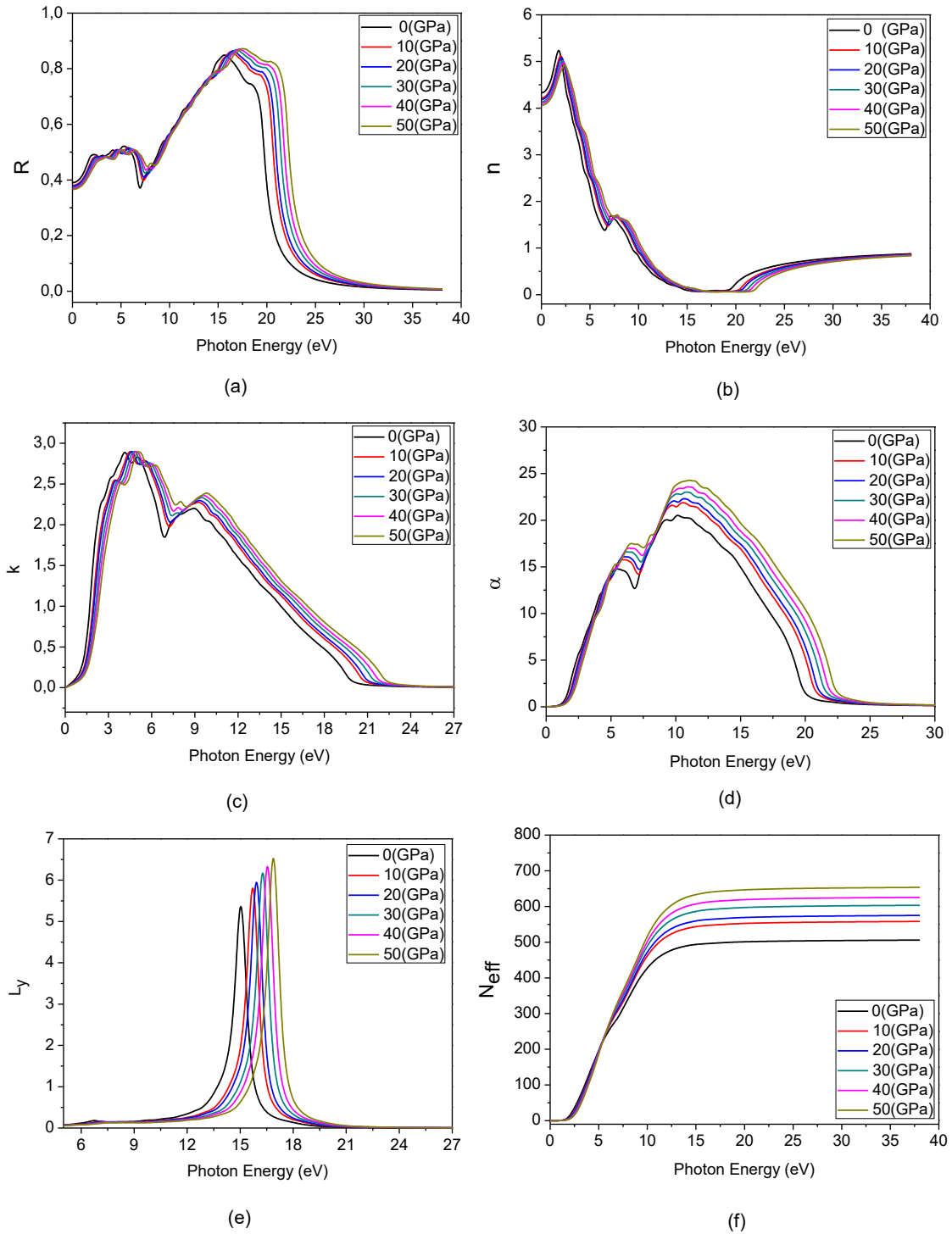
Figure 5. (a) Reflectivity (R), (b) refractive index, (c) extinction coefficient (k), (d) absorption coefficient (α), (e) energy loss function for volume (L_V), (f) effective number of valence electrons per unit cell (N_{eff}).

Some fundamental optical constants were given in Figure 5. The characteristic of the reflectivity can be seen in Figure 5 (a). The static refractive index of CoAsS was 4.33, 4.22, 4.19, 4.14, 4.10 and 4.06 for P=0, 10, 20, 30, 40 and 50 GPa, respectively. The local minimum part of the extinction coefficient corresponds to the phonon energy interval of the negative parts of the real component of dielectric constant. Loss function refers to the energy loss of a fast electron crossing

over the crystal. The peak of the energy loss function for volume (L_V) is related with the plasma oscillations with ω_p plasma frequency, which also corresponds to the negative values of the ε_1. N_{eff} specifies the contribution which was done to optical functions during the transition between the electronic bands and reaches to the saturation level (504.07) at around 15 eV. After this level there were no any transitions between the electronic bands.

3.4. Elastic properties

In order to analyze the elastic properties such as bulk modulus, shear modulus, Young modulus etc, first of all the elastic constants have to be calculated. Elastic constants are the components of elastic matrix. Elastic matrix has 36 components. Actually, elastic constants are rank four tensors with 81 components (C_{klmn}) but by using a matris notation four indices can be decreased to 2 indices (C_{ij}) and 81 components decrease to 36 components by the help of the symmetry of crystals. Additionally, cubic structures has extra symmetries, therefore, in the cubic structures elastic matrix has just three components, namely, C_{11}, C_{12}, C_{44}.

$$\begin{pmatrix} C_{11} & C_{12} & C_{13} & C_{14} & C_{15} & C_{16} \\ C_{21} & C_{22} & C_{23} & C_{24} & C_{25} & C_{26} \\ C_{31} & C_{32} & C_{33} & C_{34} & C_{35} & C_{36} \\ C_{41} & C_{42} & C_{43} & C_{44} & C_{45} & C_{46} \\ C_{51} & C_{52} & C_{53} & C_{54} & C_{55} & C_{56} \\ C_{61} & C_{62} & C_{63} & C_{64} & C_{65} & C_{66} \end{pmatrix} \rightarrow \begin{pmatrix} C_{11} & C_{12} & C_{12} & 0 & 0 & 0 \\ . & C_{11} & C_{12} & 0 & 0 & 0 \\ . & . & C_{11} & 0 & 0 & 0 \\ 0 & 0 & 0 & C_{44} & 0 & 0 \\ 0 & 0 & 0 & 0 & C_{44} & 0 \\ 0 & 0 & 0 & 0 & 0 & C_{44} \end{pmatrix}$$

The values of these elastic components are given in Table 4 with respect to the applied pressure values.

Table 4. The values of C_{11}, C_{12} and C_{44} according to the pressure values

Pressure (GPa)	C_{11} (GPa)	C_{12} (GPa)	C_{44} (GPa)
0	299.32	41.20	103.29
10	401.49	52.83	122.81
20	470.58	67.21	141.74
30	557.05	78.89	156.33
40	603.11	90.94	169.68
50	595.71	93.23	172.80

If the material is mechanically stable it has to obey to Born Stability Criterias. These criterias changes according to the crystal structure of the material (Mouhat, 2014). For cubic structure this criteria is as follows;

$$C_{11} - C_{12} > 0 \, ; C_{11} + 2C_{12} > 0 \, ; C_{44} > 0 \tag{1}$$

As seen from Table 4, our calculated values for all pressure values satisfied the criteria which confirmed that cubic CoAsS was mechanically stable.

Afterwards, we computed the values of the Bulk modulus (B) and Shear Modulus (G) with three different approximations that are namely Voight, Reuss and Hill. Then we computed Yound module (E), Poisson's coefficients (v) and Zener anisotropy factor (A) for all pressure values (Table 5). As seen from Table 5, the bulk modulus values with respect to these approximations were calculated as equal to each other.

Table 5. Values of some elastic features with respect to pressure values.

Pressure (GPa)	B_R (=B_V) (=B_{VRH}) (GPa)	G_V (GPa)	G_R (GPa)	G_{VRH} (GPa)	E (GPa)	ν (-)	K (-)	A
0	127.24	113.59	112.25	112.92	261.43	0.15	1.12	0.800
10	169.04	143.41	139.27	141.34	331.60	0.17	1.19	0.705
20	201.66	165.71	160.86	163.29	385.75	0.18	1.23	0.703
30	238.28	189.42	181.45	185.44	441.73	0.19	1.28	0.654
40	261.66	204.24	196.15	200.20	478.55	0.20	1.31	0.663
50	260.72	204.17	197.45	200.81	479.37	0.19	1.30	0.688

The ratio of bulk modulus and shear modulus (K) gives the fragility of that material. The smaller values than the critical value of K e.i. 1.75, are fragile materials. We found this ratio as 1.12 for the ground state and 1.30 for the P=50 GPa, it showed that cubic CoAsS was a fragile material. Also the critic value of Poisson ratio is $0.\bar{3}$. The smaller values indicates that materials have fragile property. Since our calculated values of Poisson ratio's for all pressure values were smaller than $0.\bar{3}$, so this also provided that our material was fragile. The anisotropy factor (A) points that the elastic anisotropy of the materials. Our calculated values were between 0.800 and 0.688 that demonstrates that cubic CoAsS has elastic anisotropy.

3.5. Thermodynamic properties

To investigate the thermodynamic features of cubic CoAsS mineral, the Helmholtz free energy ΔF, the internal energy ΔE, the constant-volume specific heat C_V and the entropy S were calculated as a function of temperature and given in Figure 6.

(a)

(b)

(c)

(d)
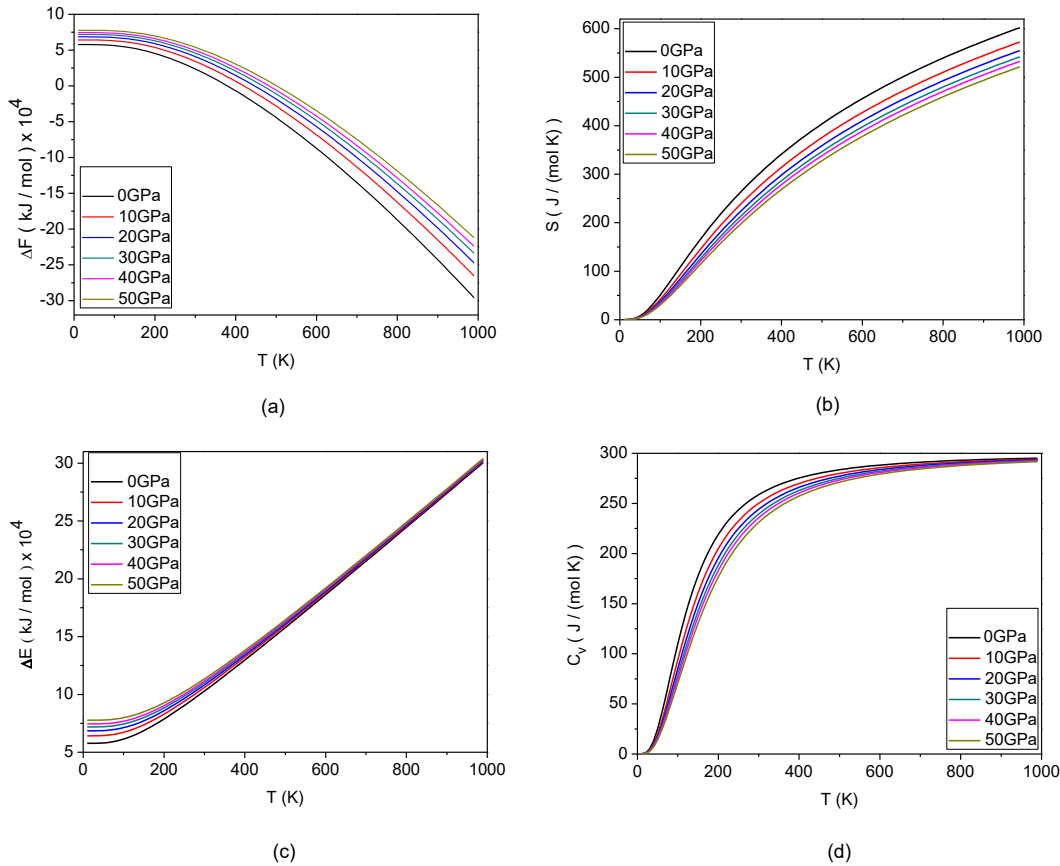
Figure 6. Some thermodynamic properties of cubic CoAsS such as (a) Helmholtz Free energy ΔF, (b) Entropy S, (c) internal energy ΔE and (d) constant- volume specific heat C_V.

As seen from Figure 6, the free and the internal energies were different from zero at zero temperature, so it was clear that at zero point oscillations occured. The value of free energy was 5.789 $x10^4$ k J /mol and the value of internal energy was $5.796x10^4$ k J /mol at zero temperature for the ground state. These values were very close to each other as expected. At the same temperature point the values of both energies were increasing as ingreasing the pressure (Figures 6 (a) and (c)). However as the pressure were increasing the entropy and the constant-volume specific heat decreased. Specific heat approached a limit value 295.11 J/mol K at 914.96 K.

4. Conclusions

The approach of this study was to figure out some physical properties of cubic CoAsS mineral such as structural, electronic, optical, elastic and thermodynamic properties in the ground state and the influence of pressure on those properties. The lattice parameters for all pressure values were calculated and one for the ground state was compared with the literature, which was given a good agreement. Afterwards the electronic band structure and the density of states were computed and plotted, which showed that this material was a semiconductor with an indirect band gap. We found out the optical properties of cubic CoAsS under pressure. It was found that this material was elastically fragile and structurally deformed at around 40GPa and higher pressure values as also noticed in the electronic properties. Last of all the Helmholts free energy, internal energy, entropy and constant volume specific heat were investigated for the ground state and under pressures. These calculations were performed for the first time that is why we could not compared our results with the literature. We believe that this study will be a guide for new further studies on cubic CoAsS mineral.

References

Bayliss, P. (1982). A further crystal structure refinement of cobaltite. *American Mineralogist,* 67, 1048-1057.

Erdinc, B., Secuk, M. N., Aycibin, M., Gulebagan, S. E., Dogan, E. K. & Akkus, H. (2015). Ab-initio calculations of physical properties of alkali chloride XCl (X = K, Rb and Li) under pressure. *Computational Condensed Matter,* 4, 6-12. doi:10.1016/j.cocom.2015.05.001

Ertseva, L. N & Tsymbulov, L. B. (2002). On transformations of iron, nickel, and cobalt arsenides and sulfoarsenides under thermal treatment in various media. *Russian Journal of Applied Chemistry,* 75 (10), 1547-1556.

Fleet, M. E. & Burns, P. C. (1990). Structure and twinning of cobaltite. *Canadian Minerologist,* 28, 719-723.

Fuch, M. & Scheffler, M. (1999). Ab initio pseudopotentials for electronic structure calculations of poly-atomic systems using density-functional theory. *Computer Physics Communications,* 119, 67-98. doi:10.1016/S0010-4655(98)00201-X

Gao, M. R., Zheng, Y. R., Jiang, J. & Yu, S. H. (2017). Pyrite-type nanomaterials for advanced electrocatalysis. *Accounts of Chemical Research,* 50, 2194−2204. doi:10.1021/acs.accounts.7b00187

Gonze, X., Beuken, J. M., Caracas, R., Detraux, F., Fuchs, M., Rignanese, G. M., Sindie, L., Verstrate, M., Zerah, G., Jollet, F., Torrent, M., Roy, A., Mikami, M., Ghosez, P., Raty, J. Y. & Allan, D. C. (2002). First-principles computation of material properties: the ABINIT software Project. *Computational Materials Science,* 25, 478-492. doi:10.1016/s0927-0256(02)00325-7

Jain A., Ong S. P., Hautier, G., Chen, W., Richards, W. D., Dacek, S., Cholia, S., Gunter, D., Skinner, D., Ceder, G. & Persson, K. A. (2013). Commentary: The materials project: A materials genome approach to accelerating materials innovation. *APL Materials,* 1(1), 011002. doi:10.1063/1.4812323

Kaura, P. & Bera, C. (2017). Effect of alloying on thermal conductivity and thermoelectric properties of CoAsS and CoSbS. *Physical Chemistry Chemical Physics*,19, 24928-24933.

Kohn, W. & Sham, L. J. (1965). Self-consistent equations including exchange and correlation effects. *Physical Review,* 140, A1133. doi:10.1103/PhysRev.140.A1133

Liu, L. & Zhuang, H. L. (2019). Single-layer ferromagnetic and piezoelectric CoAsS with pentagonal structure. *APL Materials,* 7, 011101. doi:10.1063/1.5079867

Monkhorst, J. H. & Pack, J. D. (1976). Special points for Brillouin-zone integrations. *Physical Review B,* 13, 5188-5192. doi:10.1103/PhysRevB.13.5188.

Mosselmans, J. F. W., Pattrick, R. A. D., van der Laan, G., Charnock, J. M., Vaughan, D. J., Henderson, C. M. B. & Garner, C. D. (1995). X-ray absorption near-edge spectra of transition metal disulfides FeS2 (pyrite and marcasite) COS2, NiS2 and CuS2, and their isomorphs FeAsS and CoAsS. *Physics and Chemistry of Minerals,* 22, 311-317. doi:10.1007/bf00202771

Mouhat, F. & Coudert, F. X. (2014). Necessary and sufficient elastic stability conditions in various crystal systems. *Physical Review B*, 90, 224104. doi:10.1103/PhysRevB.90.224104

Okoye, C. M. I. (2004). Investigation of the pressure dependence of band gaps for silver halides within a first-principles method. *Solid State Communications*, 129, 69-73. doi:10.1016/j.ssc.2003.09.014

Payne, M. C., Teter, M. P., Allan, D. C., Arias, T. A. & Joannopoulos, J. D. (1992). Iterative minimization techniques for *ab initio* total-energy calculations: molecular dynamics and conjugate gradients. *Review of Modern Physics,* 64, 1045-1097. doi:10.1103/RevModPhys.64.1045

Perdew, J. P., Chevary, J. A., Vosko, S. H., Jackson, K. A., Pederson, M. R., Singh, D. J., & Fiolhais, C. (1992). Atoms, molecules, solids, and surfaces: Applications of the generalized gradient approximation for exchange and correlation. *Physical Review B,* 46, 6671-6687. doi:10.1103/PhysRevB.46.6671

Pielnhofer, F., Schöneich, M., Lorenz, T., Yan, W., Nilges, T., Weihrich, R. & Schmidt, P. (2015). A rational approach to IrPTe – DFT and CalPhaD studies on phase stability, formation, and structure of IrPTe. *Zeitschrift für anorganische Chemie,* 641 (6), 1099–1105. doi:10.1002/zaac.201500149

Troullier, N. & Martins, J. L. (1991). Efficient pseudopotentials for plane-wave calculations. *Physical Review B,* 43, 1993-2006. doi:10.1103/PhysRevB.43.1993

Weihrich, R., Kurowski, D., Stückl, A. C., Matar, S. F. Rau, F. & Bernerta, T. (2004). On the ordering in new low gapsemiconductors: PtSnS, PtSnSe, PtSnTe. Experimental and DFT studies. *Journal of Solid State Chemistry*, 177, 2591–2599. doi:10.1016/j.jssc.2004.03.031